NUMERICAL INVESTIGATION OF A HIGHLY EFFECTIVE HYSTERETIC NONLINEAR ENERGY SINK IN SHOCK MITIGATION

George C. Tsiatas[1] and Aristotelis E. Charalampakis[2]

[1]Department of Mathematics
University of Patras
Rio, GR-26504, Greece
e-mail: gtsiatas@math.upatras.gr; web page: http://www.math.upatras.gr/~gtsiatas/

[2]Department of Civil Engineering
National Technical University of Athens
Athens, GR-15773, Greece
e-mail: achar@mail.ntua.gr; web page: http://charalampakis.com

Keywords: Nonlinear Energy Sink, Tuned Mass Damper, Seismic response mitigation, Hysteresis, Negative stiffness, Bouc-Wen.

Abstract. *In this paper, the behavior of the novel Hysteretic Nonlinear Energy Sink (HNES) in seismic response mitigation is investigated. HNES is a modification of a type-I NES device which, in addition to the essential nonlinear cubic element, also incorporates a Bouc-Wen type hysteretic element and a negative stiffness element. The response reduction of a two-degree-of-freedom model of a shear building is studied against a strong ground motion using a HNES, a type-I NES and a traditional Tuned Mass Damper (TMD). For each case, the optimum configuration which minimizes the maximum absolute displacement of the top floor is determined using Differential Evolution, a robust metaheuristic algorithm. It is shown that HNES performance is vastly superior to both NES and TMD, with the additional advantage of insensitivity to changes in structural characteristics.*

1 INTRODUCTION

The concept of passive vibration control by means of a mass damper was proposed by Watts as early as 1883 [1] and patented by Frahm [2], who used the term "*dynamic vibration absorber*". A classical engineering device implementing this concept is the Tuned Mass Damper (TMD), which is attached to a primary vibrating system in order to suppress undesirable vibrations. The device consists of a small mass m, a linear spring element k and a viscous damper c and its natural frequency is tuned in resonance with the fundamental mode of the primary system. When tuned properly, a large amount of the structural vibrating energy is transferred from the primary system to the TMD and then dissipated by damping.

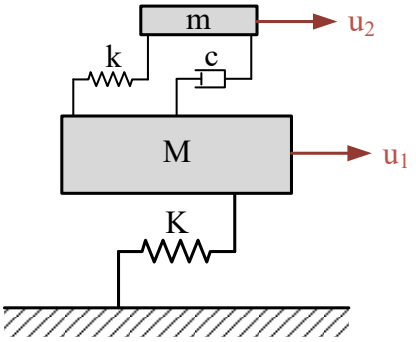

Figure 1: Schematic representation of a dynamic vibration absorber for an undamped SDoF system as suggested by Den Hartog [3].

Since Den Hartog [3] first proposed an optimal design theory for the TMD for an undamped single-degree-of-freedom (SDoF) structure (Figure 1), the TMD has been employed on a vast array of systems, with skyscrapers being among the most interesting ones [4–6]. Apart from buildings, recent studies also include the use of TMDs for vibration absorption in seismic or other forms of excitation of bridge structures [7].

Even though TMDs are very efficient when tuned properly, they possess certain drawbacks. First, their efficacy is subject to errors in the initial estimate of the natural frequency. They are also rather sensitive to detuning [6,8], caused by common time-related processes, such as creep, or during a major seismic event due to the accumulated inelastic deformations of the structure. Researchers have attempted to mitigate their sensitivity by using alternative configurations, e.g., by stacking multiple TMDs together [9] or by introducing active control elements, as in Active Mass Dampers (AMDs) [10]. Nevertheless, little progress has been achieved regarding the detuning of a passive TMD device. In addition, a large oscillating mass is generally required in order to achieve significant vibration reduction, rendering its construction and placement rather difficult in real-life situations.

In light of the above, the use of essentially nonlinear (i.e., non-linearizable) attachments to the primary oscillating system has gained tremendous attention by researchers. When properly designed, these attachments act, in essence, as Nonlinear Energy Sinks (NESs), i.e., they passively absorb energies generated by transient disturbances in the primary oscillating system to which they are weakly attached [11]. This broadband, one-way directed transfer of energy from the primary oscillator to the nonlinear attachment, termed Targeted Energy Transfer (TET), is realized in NESs of various designs [12]. Apart from their performance, the most important advantage of NESs over TMDs is that the former do not need to be fine-tuned to a particular frequency, as they absorb energy at a wider range of frequencies [13].

In total, seven types of NESs have been proposed so far. In Type I, II and III, an essentially nonlinear cubic spring has been employed with linear (Type I and III) or nonlinear (Type II) damping [14–16]. In Type IV, a rotating NES has been introduced coupled to a primary linear oscillator [17,18], whereas Type V and VI designs are devoted to strongly nonlinear vibro-impact coupling [11,19,20]. In Type VII, a negative stiffness element is employed [21], which is proved to considerably enhance the NES performance for passive energy pumping and rapid local energy dissipation.

The introduction of both rate-independent hysteresis and negative stiffness into a Type I NES has recently been investigated in shock mitigation [22]. The resulting NES, termed Hysteretic Nonlinear Energy Sink (HNES), has proved to exhibit exceptional robustness and energy dissipation merits. In this paper, three passive devices, i.e. a HNES, a type-I NES and a TMD, are optimized for the seismic response mitigation of a two-degree-of-freedom model of a shear building. The optimum properties of each device which minimize the maximum absolute displacement of the top floor are determined using Differential Evolution, a robust metaheuristic algorithm. It is shown that the performance of HNES is vastly superior, while it maintains a significant performance level even when drastic changes in the structural characteristics occur.

2 MODEL STRUCTURE

A two-degree-of-freedom shear building is studied (Figure 2), in seismic mitigation. The structure is designed to have natural frequencies similar to those of a typical midrise steel structure and has been investigated in detail in [23]. The structural properties are given in Table 1, resulting in first and second natural frequencies of 1.63 and 4.56 Hz, respectively. The damping in the model is set at 2% in each mode.

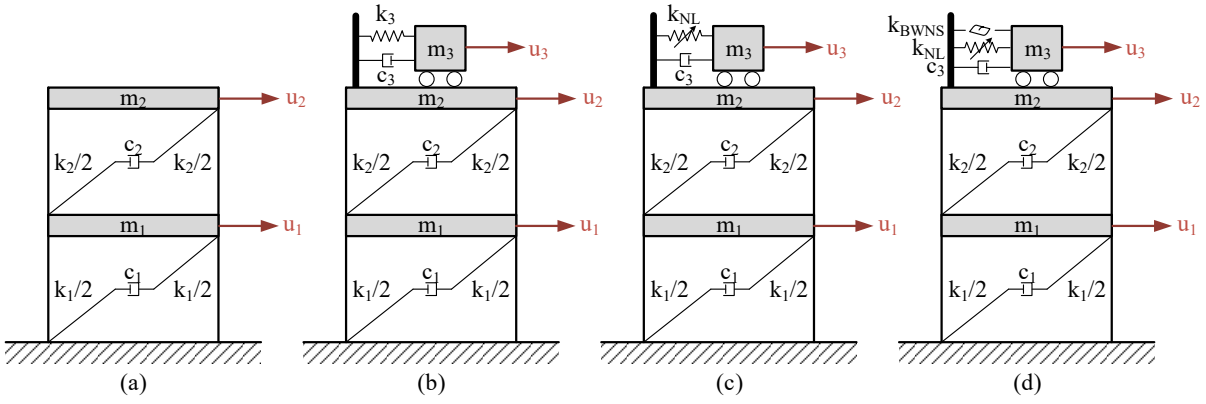

Figure 2: Structural configurations (a) unprotected structure (b) structure with TMD (c) structure with NES (d) structure with HNES

m_1	24.3 kg

k_1	6820 N/m
c_1	6.306 Ns/m
m_2	24.2 kg
k_2	8220 N/m
c_2	16.492 Ns/m
m_3	$\mu(m_1+m_2)$
μ	5%

Table 1: Structural properties

3 DESIGN GROUND MOTION

The ground acceleration record used in this study belongs to the 1999 Athens earthquake, matched to the EC8 Type-1 response spectrum on type B soil, with PGA = 0.36 g and 2% damping. The matching was performed based on the wavelets algorithm [24,25] using the SeismoMatch computer software [26]. The original and matched spectra are shown in Figure 3.

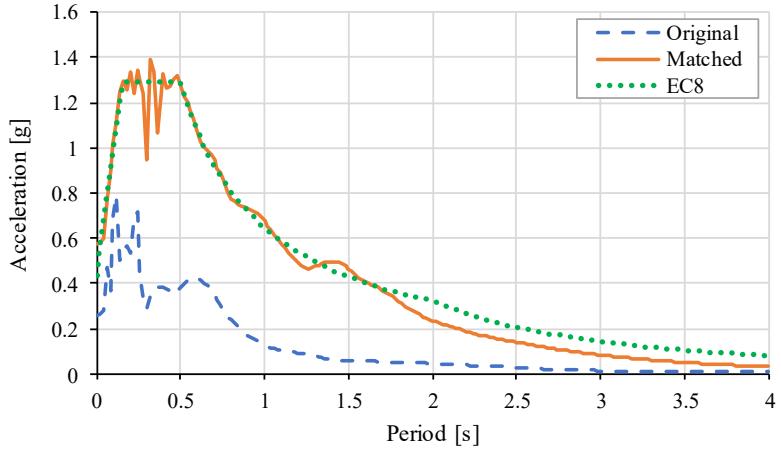

Figure 3: Design ground motion spectrum

4 HYSTERETIC NONLINEAR ENERGY SINK (HNES)

The HNES employs a rate-independent hysteretic element, a linear elastic spring of potentially negative stiffness, a viscous damper and a cubic nonlinear spring [22]. These are described in brief below.

4.1 Hysteretic Element

The Bouc-Wen model, introduced by Bouc [27] and extended by Wen [28], is employed to describe rate-independent hysteresis. The model utilizes internal (non-measurable) hysteretic variables which follow suitable differential equations. In a single-degree-of-freedom system, the hysteretic force is expressed by

$$F_{BW}(t) = a\,k\,x(t) + (1-a)k\,D\,z(t) \tag{1}$$

where, x(t) is the time history of the displacement, k>0 is the initial stiffness, D>0 is the yield displacement, and z(t) is a dimensionless hysteretic variable which is governed by the differential equation

$$\dot{z} = -\left(\beta\,\mathrm{sgn}(z\,\dot{x}\right) \tag{2}$$

in which n>0 is the exponential parameter, governing the abruptness of transition between pre- and post-yield response, and sgn() is the signum function. Parameter *a* controls the ratio of post to pre-yield stiffness, while the dimensionless parameters A, β and γ control the shape and size of the hysteretic loop [29]. For reasons of model consistency, the constraints A=β+γ=1 are imposed which simplify the model without limiting its capabilities [30–33]. As a result, z takes values in the range [-1,1], with ±1 meaning full yield in the positive/negative direction.

Based on Eq. (1), the model can be visualized as two springs connected in parallel, i.e. a linear elastic and a purely hysteretic spring, with

$$F_{BW}^{el}(t) = a\,k\,x(t) \tag{3}$$

and

$$F_{BW}^{h}(t) = (1-a)k\,D\,z(t), \tag{4}$$

respectively. The combined response is shown in Figure 4.

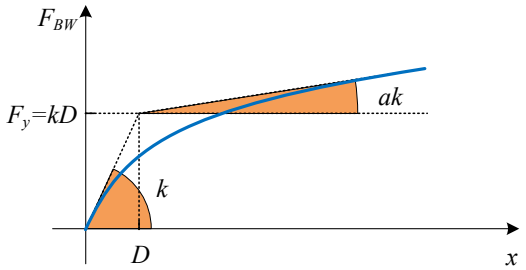

Figure 4: Response of Bouc Wen model under displacement-controlled monotonic loading

4.2 Negative Stiffness Element

The idea of employing negative stiffness springs, or 'anti-springs', for the absorption of oscillations can be traced in aeronautical engineering and the innovative work by Molyneaux [34]. This idea was extended significantly by Platus [35]. Apart from pre-compressed springs, physical implementation of negative stiffness elements can be achieved by beams, slabs or shells in post-buckled arrangements, inverse pendulum systems, etc. Some interesting implementations of such non-linear isolation systems can be found in the works of Winterflood et al. [36], Virgin et al. [37], Liu et al. [38], Antoniadis et al. [39], and others.

Instead of introducing an additional negative stiffness element, a simplest approach has recently been proposed [22] which involves the already present linear elastic spring of the Bouc-Wen model. This spring can obtain negative stiffness for negative values of parameter *a*, leading to a true softening behavior which, however, is not related to damage of any kind. This approach allows for a seamless investigation of the HNES' behavior for both positive and negative values of *a*. In this regard, the stiffness of the Bouc-Wen model is indicated as k_{BWNS} in Figure 2d, to indicate potentially negative stiffness.

4.3 Combined response

The HNES also includes a cubic nonlinear spring and a viscous damper, as in a Type-I NES. The combined response is shown in Figure 5. Note the (always) positive initial stiffness, which ensures stability in spite of the negative stiffness spring, as well as the cubic nonlinear element which can be used to restrict the stroke of HNES within feasible values.

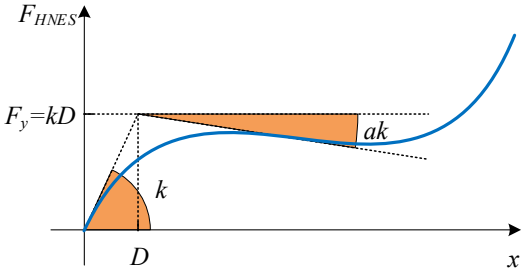

Figure 5: Combined response of HNES springs under displacement-controlled monotonic loading

5 SYSTEM DYNAMICS

Assuming that u_i is the displacement associated with mass m_i, the equations of motion take the form:

$$m_1 \ddot{\quad} \quad \cdot \quad \cdot \quad \cdot \quad \ddot{\quad}, \tag{5}$$

$$m_2 \ddot{\quad} \quad \cdot \quad \cdot \quad \cdot \quad \cdot \quad \ddot{\quad}, \tag{6}$$

$$m_3 \ddot{\quad} \quad \cdot \quad \cdot \quad \ddot{\quad}, \tag{7}$$

where, $\ddot{\quad}$ is the ground acceleration and F_{S3} is the restoring force of the configuration connecting mass m_3 to the structure. In case of a TMD,

$$F_{S3} = k_3 \left(u_3 - u_2\right), \tag{8}$$

while in case of a type-I NES

$$F_{S3} = k_{NL} \left(u_3 - u_2\right)^3. \tag{9}$$

In case of the proposed HNES configuration, a Bouc-Wen type spring, described by Eqs. (1) and (2), is connected in parallel to the cubic nonlinear spring, producing a total restoring force given by:

$$F_{S3} = k_{NL} \left(u_3 - u_2\right)^3 + a\, k_3 \left(u_3 - u_2\right) + \left(1-a\right) k_3\, D\, z\,. \tag{10}$$

Equations (2), (5)-(7) and (10) can be cast in state-space form with zero initial conditions, as follows

$$\begin{Bmatrix} x_1 = u_1 \\ x_2 = \dot{\quad} \\ x_3 = u_2 \\ x_4 = \dot{\quad} \\ x_5 = u_3 \\ x_6 = \dot{\quad} \\ x_7 = z \end{Bmatrix}, \qquad \begin{Bmatrix} \Delta_2 = x_3 - x_1 \\ \Delta_3 = x_5 - x_3 \\ \dot{\quad} \quad c_2 \\ \dot{\quad} \quad c_4 \\ F_{S3} = k_{NL}\Delta_3^{\,3} + a\, k_3\, \Delta_3 + \left(1-a\right) k_3\, D\, x_7 \\ \dot{\quad} \\ \dot{\quad} \quad \dfrac{+ k_2\Delta_2 - c_1 x_2 + c_2 \dot{\quad}}{m_1} \ddot{\quad} \\ \dot{\quad} \\ \dot{\quad} \quad \dfrac{{}_2 + F_{S3} - c_2 \dot{\quad} \quad \cdot \quad}{m_2} \ddot{\quad} \\ \dot{\quad} \\ \dot{\quad} \quad \dfrac{- c_3 \dot{\quad}}{m_3} \ddot{\quad} \\ \dot{\quad} \quad - |x_7|^n \left(\gamma\, sign\left(\dot{\quad} \quad\right)\right) \end{Bmatrix} \tag{11), (12}$$

The above system can be integrated numerically using e.g. Runge-Kutta 4th - 5th order integrator with adaptive time step, or with another appropriate technique. Based on appropriate selection of its parameters, the system can produce the response of all cases shown in Figure 2. In particular, for very small values of m_3 one obtains the response of the unprotected structure; for k_{NL}=0 and a=1 the cubic non-linear element as well as the hysteretic spring of Bouc-Wen are disabled, producing the response of a TMD; and, finally, for k_3=0 the whole Bouc-Wen element is disabled, producing a type-I NES. By allowing these parameter values in the optimization procedure, the proposed HNES configuration is therefore able of producing a proper superset of responses with regard to both the TMD and type-I NES. It will be proved that the optimized HNES configuration indeed exhibits superior performance, with the additional advantage of insensitivity with respect to changes in the structural characteristics.

6 STATEMENT OF THE OPTIMIZATION PROBLEM

In this work, the maximum absolute displacement of the top floor is used as objective function. Thus, the optimization problem is to minimize max(abs(u_2(t))) subject to the side constraints of the active design variables given in Table 2. In order to reduce the complexity of the optimization problem, the following parameters are known to have little sensitivity and were therefore fixed to reasonable values: n=2 (smooth transition from elastic to post-elastic branch), β=γ=0.5 (unloading branches are straight lines).

	TMD (k_{NL}=0, a=1)			Type-I NES (k_3=0)			HNES		
#	Design variable	Lower bound	Upper bound	Design variable	Lower bound	Upper bound	Design variable	Lower bound	Upper bound

1	c_3 [Ns/m]	0	20	c_3 [Ns/m]	0	20	c_3 [Ns/m]	0	5
2	k_3 [N/m]	0	1000	k_{NL} [N/m^3]	0	10000	k_3 [N/m]	0	1000
3							D [m]	0.01	1
4							a [-]	-1	1
5							k_{NL} [N/m^3]	0	10000

Table 2: Side constraints of design variables

7 OPTIMIZATION METHOD

The optimum parameter values for all cases (Figure 2b - Figure 2c) has been determined by a robust metaheuristic algorithm called Differential Evolution (DE). The algorithm was introduced by Storn and Price [40] and an early version was initially conceived under the term "Genetic Annealing" [41]. In classic DE, usually denoted "rand/1/bin", a population of P individuals is randomly dispersed within the design space, as

$$\begin{aligned} &\mathbf{x}_L \le \mathbf{x}_{i,0} \le \mathbf{x}_U \ \ \forall i \in \{1,2,...,P\} \\ &\mathbf{P}_{\mathbf{x},g} = \left(\mathbf{x}_{i,g}\right),\ i \in \{1,2,...,P\},\ g \in \{0,1,...,g_{\max}\} \\ &\mathbf{x}_{i,g} = \left(x_{j,i,g}\right),\ j \in \{1,2,...,ND\} \end{aligned} \tag{13}$$

where $\mathbf{P}_{\mathbf{x},g}$ = array of P vectors (solutions); $\mathbf{x}_{i,g}$ = ND-dimensional vector representing a candidate solution; g_{max} = maximum number of generations; i = index for vectors, g = index for generations, j = index for design variables; and the parentheses indicate an array. At each generation g, a mutated population $\mathbf{P}_{\mathbf{v},g}$ is formed based on the current population $\mathbf{P}_{\mathbf{x},g}$, as

$$\mathbf{v}_{i,g} = \mathbf{x}_{r0,g} + F\left(\mathbf{x}_{r1,g} - \mathbf{x}_{r2,g}\right) \tag{14}$$

where, r_0, r_1, and r_2 are mutually exclusive random integers in {1, 2, …, P}, which are also different from index i; $\mathbf{x}_{r0,g}$ = base vector; and F = a scalar parameter. After using Eq. (14), design variables are reset to their respective bounds in case a mutated solution moves out of the initial design space. Next, a trial population $\mathbf{P}_{\mathbf{u},g}$ is formed, consisting of individuals created from the parent and mutated populations, as

$$\mathbf{u}_{i,g} = \left(u_{j,i,g}\right) = \begin{cases} v_{j,i,g}, & \text{if } \left(r \le C_r \text{ or } j = j_{rand}\right) \\ x_{j,i,g}, & \text{otherwise} \end{cases} \tag{15}$$

where, j_{rand} = a random index in {1, 2, …, P} that ensures that at least one design variable will originate from the mutant vector $\mathbf{v}_{i,g}$; and C_r = a scalar parameter in the range [0,1]. The final step of the algorithm is a greedy selection criterion, which for minimization problems is expressed as

$$\mathbf{x}_{i,g+1} = \begin{cases} \mathbf{u}_{i,g}, & \text{if } f\left(\mathbf{u}_{i,g}\right) \le f\left(\mathbf{x}_{i,g}\right) \\ \mathbf{x}_{i,g}, & \text{otherwise} \end{cases} \tag{16}$$

The above-described classic DE implementation usually demonstrates stronger exploration capability and thus is more suitable for solving multimodal problems [40]. Following recommendations in [41], F = 0.5 while a high value of C_r = 0.9 is expected to perform well with non-separable functions. The population size is set as P = 50 for all problems.

8 RESULTS AND DISCUSSION

The best results out of 10 independent runs with different random seeds (per case) are summarized in Table 3. Regarding HNES, it is immediately noted that the optimization process was guided to the removal of the viscous damper (c_3=0). In addition, the lower bound of D was selected (0.01), which means that a small yield force F_y=k_3D was proved to be beneficial.

The objective values (i.e., max(abs(u_2))) are summarized in Table 4. Compared to the response of the unprotected structure, it is shown that HNES achieves a reduction of 65.49%, i.e. more than double the reduction achieved with NES (30.71%) and almost three times the reduction achieved with TMD (23.63%). Next, a stiffness reduction is imposed in both k_1 and k_2, to account for potential deterioration effects during the life cycle of the structure. Keeping the optimum parameters of Table 3, the calculated objective values indicate that HNES maintains a significant level or performance, e.g. it still achieves a 29.13% reduction even if the column stiffnesses are reduced by half. The observed behavior is vastly superior to both NES and certainly TMD.

#	TMD (k_{NL}=0, a=1)		Type-I NES (k_3=0)		HNES	
	Design variable	Optimum value	Design variable	Optimum value	Design variable	Optimum value
1	c_3 [Ns/m]	0.591	c_3 [Ns/m]	1.076	c_3 [Ns/m]	0.000
2	k_3 [N/m]	268.357	k_{NL} [N/m^3]	4115.186	k_3 [N/m]	349.475
3					D [m]	0.010
4					a [-]	-0.863
5					k_{NL} [N/m^3]	712.164

Table 3: Optimum parameter values

% stiffness reduction in k_1, k_2	Unprotected structure	TMD (k_{NL}=0, a=1)		Type-I NES (k_3=0)		HNES	
	Objective value [m]	Objective value [m]	% reduction	Objective value [m]	% reduction	Objective value [m]	% reduction
0%	0.125607	0.095928	-23.63%	0.087035	-30.71%	0.043349	-65.49%
10%	0.129114	0.114994	-10.94%	0.103143	-20.11%	0.056351	-56.36%
20%	0.139076	0.136429	-1.90%	0.122650	-11.81%	0.064349	-53.73%
30%	0.151392	0.149725	-1.10%	0.133370	-11.90%	0.086992	-42.54%
40%	0.164471	0.148314	-9.82%	0.124886	-24.07%	0.115198	-29.96%
50%	0.157517	0.157275	-0.15%	0.137996	-12.39%	0.111632	-29.13%

Table 4: Objective values and % reduction with respect to the unprotected structure

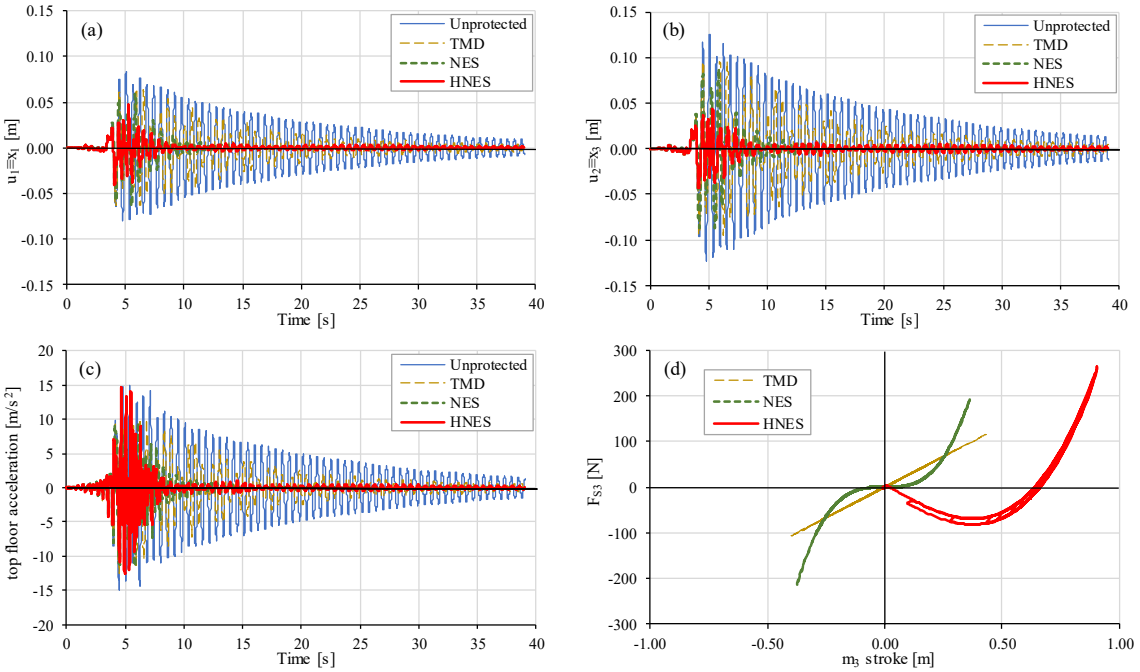

Figure 6: Response of model structure (a) bottom floor displacement u_1 (b) top floor displacement u_2 (c) top floor acceleration $\ddot{}$ (c) F_{S3} vs m_3 stroke

The response of the model structure under all alternative protection systems is shown in Figure 6. The following can be observed:

- The displacements are significantly reduced using the proposed HNES configuration, in terms of both the maximum absolute value and overall (Figure 6a,b). The reduction factors are as follows: max(abs(u_1)) 45.17%; max(abs(u_2)) 65.49%; RMS(u_1) 78.36%; and RMS(u_2) 81.70%.
- The acceleration of the top floor is comparable to the unprotected structure but only in the beginning of the event (Figure 6c). Then, the acceleration is diminished with HNES, with a reduction factor for RMS($\ddot{}$) equal to 61.55%.
- The stroke requirements with HNES are increased but not unreasonable (Figure 6d). If, however, a certain maximum level needs to be maintained, this can be taken into account in the optimization process as a

constraint.

- The hysteretic loops of HNES are very shallow due to the small yield force.
- The HNES response is almost completely displaced due to the negative stiffness spring. Restoration to the initial position is required after the event.

9 CONCLUSIONS

In conclusion, the use of HNES for seismic response mitigation is very promising and certainly deserves attention. The following can be explored (indicatively) in future research:

- The use of other objective functions in optimization e.g. RMS of displacements, top floor acceleration, etc.
- The behavior of HNES when the structure is subjected to another design ground motion as compared to the one used for optimization.
- Real-life implementations of such a device.

REFERENCES

[1] Watts, P. (1883), "On a method of reducing the rolling of ships at sea," *Transactions of the Institution of Naval Architects*, Vol. 24, pp. 165–90.

[2] Frahm, H. (US #989958, 1909.), *Device for Damping Vibrations of Bodies*,

[3] Hartog, D.J.P. (1956), *Mechanical Vibrations*, McGraw-Hill.

[4] McNamara, R.J. (1977), "Tuned Mass Dampers for buildings," Journal of Structural Division (ASCE). Vol. 103, pp. 1785–98.

[5] Luft, R.W. (1979), "Optimal Tuned Mass Dampers for Buildings," *Journal of the Structural Division*, ASCE. Vol. 105, pp. 2766–72.

[6] Rana, R. and Soong, T.T. (1998), "Parametric study and simplified design of tuned mass dampers," *Engineering Structures*, Elsevier. Vol. 20, pp. 193–204.

[7] Debnath, N., Deb, S.K. and Dutta, A. (2016), "Multi-modal vibration control of truss bridges with tuned mass dampers under general loading," *Journal of Vibration and Control*, SAGE PublicationsSage UK: London, England. Vol. 22, pp. 4121–40.

[8] Weber, B. and Feltrin, G. (2010), "Assessment of long-term behavior of tuned mass dampers by system identification," *Engineering Structures*, Elsevier. Vol. 32, pp. 3670–82.

[9] Casciati, F. and Giuliano, F. (2009), "Performance of Multi-TMD in the Towers of Suspension Bridges," *Journal of Vibration and Control*, SAGE PublicationsSage UK: London, England. Vol. 15, pp. 821–47.

[10] Soong, T.T., Reinhorn, A.M., Aizawa, S. and Higashino, M. (1994), "Recent structural applications of active control technology," *Journal of Structural Control*, John Wiley & Sons, Ltd. Vol. 1, pp. 1–21.

[11] Georgiadis, F., Vakakis, A.F., McFarland, D.M. and Bergman, L. (2005), "Shock isolation through passive energy pumping caused by non-smooth nonlinearities," *International Journal of Bifurcation and Chaos*, World Scientific Publishing Company. Vol. 15, pp. 1989–2001.

[12] Vakakis, A.F., Gendelman, O. V., Bergman, L.A., McFarland, D.M., Kerschen, G. and Lee, Y.S. (2008), *Nonlinear targeted energy transfer in mechanical and structural systems, I and II*, Springer.

[13] Boroson, E., Missoum, S., Mattei, P.-O. and Vergez, C. (2017), "Optimization under uncertainty of parallel nonlinear energy sinks," *Journal of Sound and Vibration*, Academic Press. Vol. 394, pp. 451–64.

[14] Gourdon, E., Alexander, N.A., Taylor, C.A., Lamarque, C.H. and Pernot, S. (2007), "Nonlinear energy pumping under transient forcing with strongly nonlinear coupling: Theoretical and experimental results," *Journal of Sound and Vibration*, Academic Press. Vol. 300, pp. 522–51.

[15] Quinn, D.D., Gendelman, O., Kerschen, G., Sapsis, T.P., Bergman, L.A. and Vakakis, A.F. (2008), "Efficiency of targeted energy transfers in coupled nonlinear oscillators associated with 1:1 resonance captures: Part I," *Journal of Sound and Vibration*, Academic Press. Vol. 311, pp. 1228–48.

[16] Sapsis, T.P., Vakakis, A.F., Gendelman, O., Bergman, L.A., Kerschen, G. and Quinn, D.D. (2009), "Efficiency of targeted energy transfers in coupled nonlinear oscillators associated with 1:1 resonance captures: Part II, analytical study," *Journal of Sound and Vibration*, Academic Press. Vol. 325, pp. 297–320.

[17] Gendelman, O. V., Sigalov, G., Manevitch, L.I., Mane, M., Vakakis, A.F. and Bergman, L.A. (2012), "Dynamics of an Eccentric Rotational Nonlinear Energy Sink," *Journal of Applied Mechanics*, American Society of Mechanical Engineers. Vol. 79, pp. 11012.

[18] Sigalov, G., Gendelman, O. V., AL-Shudeifat, M.A., Manevitch, L.I., Vakakis, A.F. and Bergman, L.A. (2012), "Resonance captures and targeted energy transfers in an inertially-coupled rotational nonlinear energy sink," *Nonlinear Dynamics*, Springer Netherlands. Vol. 69, pp. 1693–704.

[19] Lee, Y.S., Nucera, F., Vakakis, A.F., McFarland, D.M. and Bergman, L.A. (2009), "Periodic orbits, damped transitions and targeted energy transfers in oscillators with vibro-impact attachments," *Physica D: Nonlinear Phenomena*, North-Holland. Vol. 238, pp. 1868–96.

[20] Nucera, F., Vakakis, A.F., McFarland, D.M., Bergman, L.A. and Kerschen, G. (2007), "Targeted energy transfers in vibro-impact oscillators for seismic mitigation," *Nonlinear Dynamics*, Springer Netherlands. Vol. 50, pp. 651–77.

[21] AL-Shudeifat, M.A. (2014), "Highly efficient nonlinear energy sink," *Nonlinear Dynamics*, Springer Netherlands. Vol. 76, pp. 1905–20.

[22] Tsiatas, G.C. and Charalampakis, A.E. (2017), "A new Hysteretic Nonlinear Energy Sink (HNES)," *arXiv:170406597*,.

[23] Wierschem, N.E., Spencer, B.F., Bergman, L.A. and Vakakis, A.F. (2011), "Numerical study of nonlinear energy sinks for seismic response reduction," *The 6th International Workshop on Advanced Smart Materials and Smart Structures Technology*, Dalian, China.

[24] Abrahamson, N.A. (1992), "Non-stationary spectral matching," *Seismological Research Letters*, Vol. 63.

[25] Hancock, J., Watson-Lamprey, J., Abrahamson, N.A., Bommer, J.J., Markatis, A., Mccoyh, E. et al. (2006), "An improved method of matching response spectra of recorded earthquake ground motion using wavelets," *Journal of Earthquake Engineering*, Taylor & Francis Group. Vol. 10, pp. 67–89.

[26] SeismoSoft. (2016), "SeismoMatch - A computer program for spectrum matching of earthquake records" [Internet], www.seismosoft.com.

[27] Bouc, R. (1967), "Forced Vibrations of a Mechanical System with Hysteresis," *Proceedings of the 4th Conference on Non-Linear Oscillations*, Prague.

[28] Wen, Y.K. (1976), "Method for Random Vibration of Hysteretic Systems," *Journal of the Engineering Mechanics Division*, ASCE. Vol. 102, pp. 249–63.

[29] Charalampakis, A.E. (2010), "Parameters of Bouc-Wen hysteretic model revisited," *9th HSTAM International Congress on Mechanics*, Limassol, Cyprus.

[30] Ma, F., Zhang, H., Bockstedte, A., Foliente, G.C. and Paevere, P. (2004), "Parameter Analysis of the Differential Model of Hysteresis," *Journal of Applied Mechanics*, American Society of Mechanical Engineers. Vol. 71, pp. 342–9.

[31] Charalampakis, A.E. and Dimou, C.K. (2010), "Identification of Bouc–Wen hysteretic systems using particle swarm optimization," *Computers & Structures*, Vol. 88, pp. 1197–205.

[32] Charalampakis, A.E. and Koumousis, V.K. (2008), "On the response and dissipated energy of Bouc–Wen hysteretic model," *Journal of Sound and Vibration*, Vol. 309, pp. 887–95.

[33] Charalampakis, A.E. (2015), "The response and dissipated energy of Bouc–Wen hysteretic model revisited," *Archive of Applied Mechanics*, Springer Berlin Heidelberg. Vol. 85, pp. 1209–23.

[34] Molyneux, W.G. (1957), "Supports for Vibration Isolation," London.

[35] Platus, D.L. (1999), "Negative-stiffness-mechanism vibration isolation systems," In: Derby EA, Gordon CG, Vukobratovich D, Yoder, Jr. PR, and Zweben CH, editors. International Society for Optics and Photonics. pp. 98–105.

[36] Winterflood, J., Blair, D.G. and Slagmolen, B. (2002), "High performance vibration isolation using springs in Euler column buckling mode," *Physics Letters A*, North-Holland. Vol. 300, pp. 122–30.

[37] Virgin, L.N., Santillan, S.T. and Plaut, R.H. (2008), "Vibration isolation using extreme geometric nonlinearity," *Journal of Sound and Vibration*, Academic Press. Vol. 315, pp. 721–31.

[38] Liu, X., Huang, X. and Hua, H. (2013), "On the characteristics of a quasi-zero stiffness isolator using Euler buckled beam as negative stiffness corrector," *Journal of Sound and Vibration*, Academic Press. Vol. 332, pp. 3359–76.

[39] Antoniadis, I., Chronopoulos, D., Spitas, V. and Koulocheris, D. (2015), "Hyper-damping properties of a stiff and stable linear oscillator with a negative stiffness element," *Journal of Sound and Vibration*, Academic Press. Vol. 346, pp. 37–52.

[40] Storn, R.M. and Price, K. V. (1997), "Differential Evolution – a simple and efficient heuristic for global optimization over continuous spaces," *Journal of Global Optimization*, Kluwer Academic Publishers. Vol. 11, pp. 341–59.

[41] Price, K. V., Storn, R.M. and Lampinen, J.A. (2005), *Differential evolution : a practical approach to global optimization*, Springer.